Hepatic *Cdkal1* and reverse cholesterol transport

SeungMin Seok

The Graduate School Yonsei University

The Graduate Program of Biomedical Engineering

Hepatic *Cdkal1* and reverse cholesterol transport

Directed by Professor Sang-Hak Lee

The Master's Thesis submitted to
the Department of Graduate Program
in Biomedical Engineering,
the Graduate School of Yonsei University
in partial fulfillment of the requirements
for the degree of Master of Biomedical Engineering

Seungmin Seok

December 2023

This certifies that the master's thesis of

Seungmin Seok is approved.

_____

Thesis Supervisor: Sang-Hak Lee

_____

Thesis Committee Member #1: Jae Woo Song

_____

Thesis Committee Member #2: Chan Joo Lee

The Graduate School

Yonsei University

December 2023

ACKNOWLEDGEMENTS

석사 과정을 무사히 마칠 수 있기까지 많은 분들의 도움이 있었습니다. 이 글을 통해 감사의 인사를 전해 드리고자 합니다.

먼저 석사 학위 동안 이상학 교수님의 지도 아래, 귀중한 조언과 격려를 받을 수 있어 큰 행운이었습니다. 항상 더 나은 방향으로 나아갈 수 있도록 아낌없는 가르침을 주신 이상학 교수님께 진심으로 깊은 감사를 드립니다. 심사 과정 동안 따뜻한 관심과 진심 어린 조언을 해주신 송재우 교수님, 이찬주 교수님께도 깊은 감사의 마음을 전합니다. 그리고 학위 시작에 있어 저를 이끌어주시고 챙겨주신 정지형 교수님께도 깊은 감사를 드립니다. 교수님들의 가르침을 바탕으로 더 나은 연구자로 성장하도록 노력하겠습니다.

또한, 통찰력 있는 조언과 지도를 해주신 안수진 박사님, 입학했을 때부터 늘 챙겨주고 많이 의지했던 단비 언니, 함께 연구하며 학위 과정 동안 즐거운 추억을 쌓게 해준 현지, 지은이에게 고마움을 전합니다. 같은 실험실에서 응원해주시고 도움을 주신 최진옥 선생님, 채민경 선생님께도 감사의 인사를 전합니다. 그리고 제게 힘이 되어주고 항상 내 편이 되어준 민경이, 아낌없는 조언과 지지로 든든한 버팀목이 되어준 민숙이, 현진이, 현정이, 예지에게도 고마움을 전합니다.

마지막으로 긴 여정 동안 저를 믿고 지지해주시고 끊임없는 격려와 지원을 해주신 부모님을 비롯하여 우리 가족에게 진심으로 감사드립니다.

다시 한번 교수님들과 도움을 주신 모든 분들께 깊은 감사의 인사를 드리며 학위 과정에서 얻은 경험과 지식을 토대로 미래에 기여할 수 있는 기회를 찾아 나아가겠습니다.

석승민 올림

TABLE OF CONTENTS

LIST OF FIGURES

LIST OF TABLES

ABSTRACT

Hepatic *Cdkal1* and reverse cholesterol transport

SeungMin Seok

Graduate Program in Biomedical Engineering
The Graduate School, Yonsei University

(Directed by Professor Sang-Hak Lee)

The *Cdkal1* gene is near a locus associated with cholesterol efflux capacity, an indicator of high-density lipoprotein function and the first step of reverse cholesterol transport (RCT). Here, we investigated the effect of *Cdkal1* on RCT using a mouse model. Foam cells were treated with ^{3}H labeled cholesterol and injected intraperitoneally into mice. After 48 hours, plasma, liver, and feces were collected, and radioactivity was measured using a liquid scintillation counter.

Murine proteomic analyses were performed to identify proteins and pathways potentially relevant to the effect of *Cdkal1*. Mouse liver proteins were extracted and analyzed using liquid chromatography-mass spectrometry.

Liver-specific *Cdkal1*-deficient mice were produced by crossing *Cdkal1*$^{fl/fl}$ mice with *Alb-Cre* mice. RCT experiments revealed that *Cdkal1* deficiency affects the excretion of fecal bile acid and cholesterol, as bile acids were 17% (p=0.035) higher and cholesterol was 42% (p=0.036) higher in *Cdkal1* knockout (KO) mice compared with *Cdkal1*$^{fl/fl}$ mice.

Proteomic analysis comparing *Cdkal1* KO mice to *Cdkal1*$^{fl/fl}$ mice identified several differentially expressed proteins including CYP3A11.

In conclusion, liver-specific *Cdkal1* deficiency promoted RCT in our mouse model. Proteins potentially associated with the effect of *Cdka11* including CYP3A11 were identified by proteomic analyses. These results suggest that *Cdkal1* may be a potential therapeutic target for metabolic and atherosclerotic vascular disease.

Key words: reverse cholesterol transport, liver, proteomics, atherosclerosis

Hepatic *Cdkal1* and reverse cholesterol transport

SeungMin Seok

Graduate Program in Biomedical Engineering

The Graduate School, Yonsei University

(Directed by Professor Sang-Hak Lee)

I. INTRODUCTION

Cardiovascular diseases, including atherosclerosis, are among the leading causes of death worldwide[1]. Cholesterol efflux capacity (CEC) is a proven predictor of the degree of atherosclerosis[2]. Several studies have also confirmed the relationship between reverse cholesterol transport (RCT) and atherosclerotic cardiovascular disease[3]. RCT is a mechanism by which the body removes excess cholesterol from

surrounding tissues and transfers it to the liver for redistribution to other tissues or for removal from the gallbladder[4]. First, the intestine and liver synthesize apolipoprotein A1 (ApoA1), which travels through blood vessels to the surrounding tissues. During this process, cholesterol and some lipids interact with ApoA1, leading to the formation of high-density lipoprotein-cholesterol (HDL-C) particles. Cholesterol is transported to the liver by two pathways. In the first pathway, HDL molecules interact with the scavenger receptor class B type 1 (SR-B1) in the liver and deliver cholesterol, and in the second pathway, HDL-C molecules deliver cholesterol, especially low-density lipoprotein (LDL), to ApoB -100[5,6]. To investigate the mechanism of RCT J774 cells were radiolabeled with ^{3}H-cholesterol and treated with acetylated LDL for 48 h. Extraction of plasma and liver lipids as well as cholesterol and bile acids from feces was performed 48 hours after intraperitoneal injection of J774 foam cells. Radioactivity was measured with a liquid scintillation counter (LSC).[7,8]

CDK5 Regulatory Subunit Associated Protein 1 Like 1 (*CDKAL1*) is a protein-coding gene, and variants of *CDKAL1* are closely associated with an increased incidence of type 2 diabetes and obesity[9]. Additionally, *CDKAL1* is a known mammalian methylthiotransferase that biosynthesizes 2-methylthio-N6-threonylcarbomoyladenosine (ms2t6a) from tRNA (Lys)[10].

However, the precise role of *CDKAL1* in atherosclerotic cardiovascular disease remains unknown. Our previous genome-wide association study found that the *CDKAL1* gene is close to the locus associated with CEC[11]. Four mutations (rs117835232, rs117252933, rs118065692, and rs150434350) located in *CDKAL1* showed significant association with CEC. This association remained significant even after adjusting for HDL-C levels and other clinical variables. Therefore, our present study sought to determine whether *Cdkal1* affects RCT in mice and to identify proteins and biological pathways that likely mediate the effects of this gene.

The purpose of this study was to determine how liver-specific *Cdkal1* deficiency in mice affects RCT and to investigate factors and pathways that may be affected by *Cdkal1*. We propose a new research direction in which *Cdkal1* could be a therapeutic target for atherosclerosis.

II. MATERIALS AND METHODS

1. Animals

To induce liver-specific deficiency of the *Cdkal1* gene, we crossed *Cdkal1*$^{fl/fl}$ mice (generated from *Cdkal1*$^{fl/fl}$ sperm donated by Professor Tomizawa at Kumamoto University in Japan) with *Alb-Cre* mice (The Jackson Laboratory, Bar Harbor, ME, U.S.A.). Before the experiment, genotypes were confirmed by polymerase chain reaction (PCR) using mouse toe tissue. Liver-specific *Cdkal1* deficiency was confirmed by western blot using aliquots of the mouse liver tissue. Mouse characteristics are shown in Table 1.

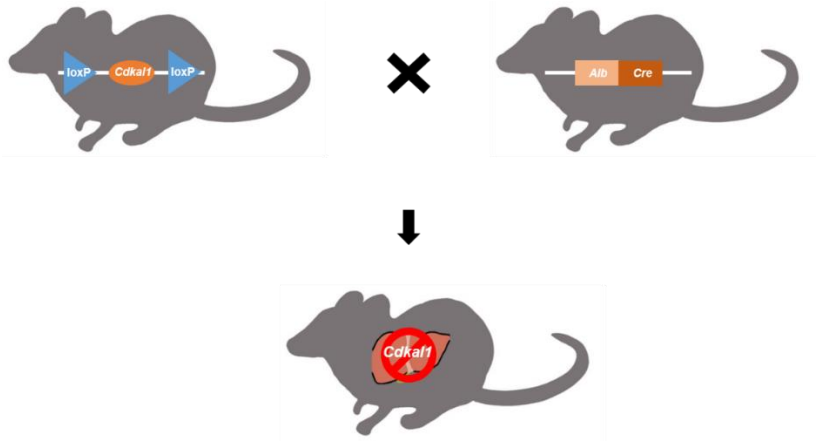

Figure 1. Generation of liver-specific *Cdkal1* deficient mouse. Mice were generated using the loxP system. For liver-specific *Cdkal1* KO, *Alb-Cre* mice were crossed with $Cdkal1^{fl/fl}$ mice.

2. Genotyping

To ascertain successful mating in mice, the toes of 4-5-week-old pups were gently clipped and stored in 1.5 ml tubes. The tube containing the tissue was centrifuged, followed by the addition of dilution buffer and DNA release buffer. The reaction took place at room temperature for 5 minutes, followed by a 2-minute reaction at 98℃. Subsequently, the mixture was cooled to room temperature, and DNA extraction was carried out, transferring only the upper DNA-containing supernatant to a new tube. For the PCR, a DNA mixture was prepared by combining

1 μl of DNA, 1 μl each of the forward and reverse primers, and 17 μl of high-temperature-sterilized and filtered distilled water (DW) in a PCR kit tube, resulting in a total volume of 20 μl. After PCR, a 100 bp DNA ladder (BIONEER, 3 μl) and the PCR-synthesized genomic DNA (10 μl) were subjected to electrophoresis to visualize the bands. The band sizes for each gene were as follows: *Cdkal1* – wild type (300 bp), fl/fl (500 bp), heterozygous (300 bp & 500 bp), and *Cre* (100 bp).

3. RCT experiment

J774 cells were cultured in Dulbecco's Modified Eagle Medium (DMEM, with 10% FBS, 1% Abs) and treated with 5 μCi/mL ^{3}H-cholesterol and 100 μg/mL acetylated low-density lipoprotein for 48 hours. Approximately 1×10^{7} cells were diluted in 500 ul of phosphate-buffered saline (PBS) or DMEM and intraperitoneally injected into mice. After 48 hours, plasma was obtained from the saphenous vein. Feces were collected once after 48 h and stored at 4 °C during the extraction of cholesterol and bile acids. Liver tissue was collected after perfusion with PBS, and 100 mg of the tissue was used for analysis. For lipid extraction from liver tissue, the Bligh and Dyer method was used[12]. Plasma, liver, and feces samples were measured for radioactivity using LSC. This study received

institutional review board approval from the animal experiment ethics committee of Yonsei University (2020-0310).

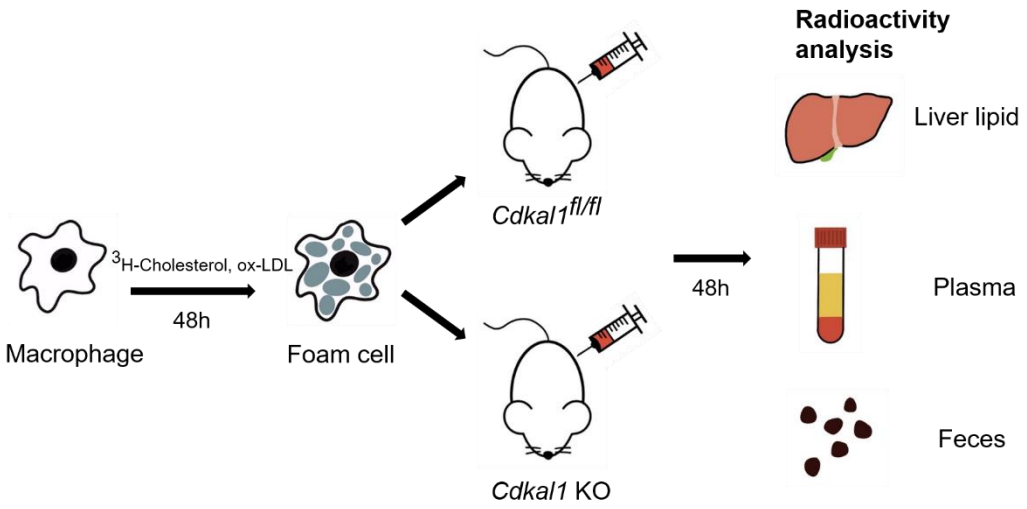

Figure 2. RCT experiment.

4. Preparation of proteins from mouse liver

Mice were anesthetized and then dissected to access the saphenous vein, from which blood was extracted. Following this, mice were perfused with PBS to obtain clean liver tissue. The largest lobe of the liver was excised and placed into a 1.5 ml tube. Following the addition of lysis buffer, the tissue was homogenized uniformly using a homogenizer. After gentle vortexing and a brief spin-down, lysates were kept on ice for 30 minutes to 1 hour. Subsequently, centrifugation was conducted at

13,000 rpm at 4 °C for 30 minutes to 1 hour. The supernatant containing proteins was collected into a sterile new tube and used in the subsequent experiments.

Impurities were removed using Detergent Removal Spin Columns & Plates (Thermo Fisher Scientific, Waltham, MA, U.S.A.). Samples were then prepared using Tryptic Digestion Kits (Thermo Fisher Scientific, Waltham, MA, U.S.A.). First, digestion buffer and reducing buffer were added, and denaturation and reduction were performed at 95 ℃ for 5 minutes. Alkylation buffer was added and samples were incubated for 20 minutes at room temperature in the dark. Digestion was performed twice using activated trypsin. Finally, guanidination was performed and trifluoroacetic acid was added to stop the reaction. The prepared samples were analyzed by liquid chromatography-mass spectrometry (LC-MS).

5. Mass spectral analysis

Tryptic digests of proteins were separated using 2-dimensional LC and 2 microliters of each sample were injected into Acclaim PEPMAP 100 (75 um*2 cm, c18, 3 um, 100 A) and PEPMAP RSLC C18 (2 um, 100 A, 75 um*50 cm) columns (Thermo Fisher Scientific, Waltham, MA, U.S.A.). Each column was equilibrated with buffer A (0.1% formic acid in DW) plus B (0.1% formic acid in acetonitrile)

and the operating flow rate was 0.3 μl/min. The nano HPLC system was coupled with a Q-EXACTIVE-Orbitrap mass spectrometer (Thermo Fisher Scientific, Waltham, MA, U.S.A.). The spray voltage was set to 2.1 kV and the temperature of the heated capillary was set to 275℃. Survey full-scan MS spectra (400–2,000 m/z) were acquired with one micro-scan at a resolution of 70,000, allowing preview mode for precursor selection and charge-state determination. MS conditions: isolation width, 1.6 m/z; normalized collision energy, 30%. Precursors with +1 charge and unassigned charge states were discarded during data-dependent acquisition and dynamic exclusion was 30 seconds.

Each LC-MS/MS file was analyzed using Proteome Discoverer 2.5 (Thermo Fisher Scientific, Waltham, MA, U.S.A.) and MAXQUANT version 1.6.5.0. A strict false discovery rate of 0.01, a relaxed false discovery rate of 0.05, and a total of 2 target values for a decoy database search were applied. All proteins were identified by two or more unique peptides.

6. RNA extraction from mouse liver and quantitative real-time PCR

The largest lobe of the mouse liver was excised and placed in a 1.5 ml tube. The tissue was homogenized uniformly using a homogenizer. Afterwards, the LYS solution included in RNA extraction kit (GeneAll Biotechnology) and 2-

mercaptoethanol (BIOSESNAG) were mixed at a ratio of 100:1 and added. After gentle vortexing and brief spin-down, the lysate was loaded onto the column included in the kit. RNA was extracted as described in the kit protocol. After quantification of total RNA using Nanodrop ND 1000, cDNA was synthesized using iScript cDNA Synesis Kit (BIO RAD, CA, USA). Gene expression was analyzed by quantitative PCR using the SYBR-Green System on a 7500 Real-Time PCR System (Applied Biosystems, CA, USA). The average cycle threshold (CT) value obtained after two measurements was used to calculate gene expression with normalization to GAPDH as a control.

7. Statistical analysis

All graphs were created using GraphPad Prism 9 (GraphPad Software Ltd, La Jolla, CA, U.S.A.) and RCT data are expressed as mean ± standard error of the mean. In RCT trials, differences between groups were assessed using permutation tests. Proteomic analysis results were analyzed with the String version 12.0 bioinformatics tool. Correlation analysis was performed using the Pearson correlation test. All analyzes were performed using R version 4.0.4 (R Foundation for Statistical Computing, Vienna, Austria). P values lower than 0.05 were considered statistically significant.

III. RESULTS

1. Characteristics of mice.

Information about the mice used in the experiments, including genotyping information, is provided in Table 1. *Cdkal1*$^{fl/fl}$ mice were used as a control. Only male mice were used in these experiments. All mice were housed under identical conditions. There were no differences between the control and experimental groups except the genotype. There was also no difference in mean body weight between control mice and *Cdkal1* KO mice.

Table 1. Characteristics of mice

	Strain	Genotype	Number	Sex	Age (weeks)	Weight (g)
Control	C57BL/6	*Cdkal1*$^{fl/fl}$	6	Male	18±6	23±5
Cdkal1 KO	C57/BL6	*Cdkal1*$^{fl/fl}$ × *Alb-Cre*	6	Male	18±6	21±6

Mean±SD. Three mice were used for proteomic analysis and six mice were used for RCT and correlation analysis.

2. Effect of hepatic *Cdkal1* deletion on RCT.

Plasma and liver radioactivity were not different between *Cdkal1*$^{fl/fl}$ mice and *Cdkal1* KO mice. In contrast, radioactivity measured in bile acids (0.81 ± 0.11 and 0.69 ± 0.04%, respectively, p = 0.035) and cholesterol (0.44 ± 0.10 and 0.31 ± 0.07%, respectively, p = 0.036) was higher in *Cdkal1* KO mice than in control mice (Figure 3). Thus, *Cdkal1* deficiency affects fecal bile acids and cholesterol excretion.

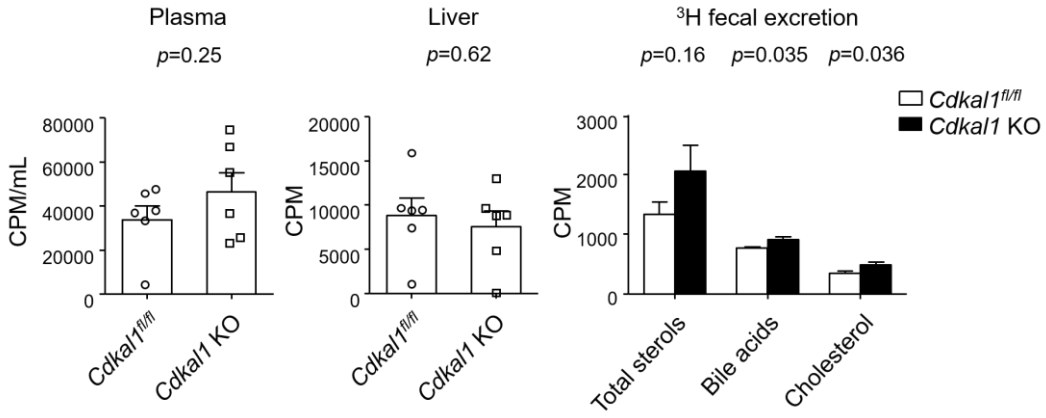

Figure 3. Effect of hepatic *Cdkal1* deletion on RCT. We determined the effect of *Cdkal1* deficiency on RCT by measuring radioactivity in plasma, liver, and feces. Analysis was conducted on the final collection of feces after 48 hours. There were no differences in activities in plasma, liver, and fecal total sterols. However, radioactivity observed in fecal bile acids and cholesterol significantly differed (permutation test; n=6-7). CPM: counts per minute.

3. Differentially expressed proteins and associated biological pathways in *Cdkal1* KO mice.

Mass spectral analysis of the extracted peptides from each sample identified 785 proteins in *Cdkal1* gene-deleted mouse livers. A total of 397 proteins were upregulated while 388 proteins were downregulated. The red dot indicates log2 fold change relative abundance ratios > 0.5 or < 0.5, and P values < 0.05 are indicated in the vertical (y-axis) and horizontal (x-axis) axes. A total of 115 proteins were significantly changed, including 48 upregulated proteins and 67 downregulated proteins.

In the case of *Cdkal1* gene-deleted mouse liver, there were relatively more up-regulated proteins. In mice with *Cdkal1* deletion, the expression of proteins such as cytochrome P450 3A11, major urinary protein 20, and small ribosomal subunit protein mS29 was increased, while the expression of proteins such as ubiquitin-conjugating enzyme E2 N, cytochrome c oxidase subunit 2 and dehydrogenase/reductase SDR family member 1 was decreased (Figure 4). In line with the observed increase in RCT in *Cdkal1* KO mice, we identified significantly changed proteins related to HDL function and metabolism. For example, CYP3A11 is highly significantly associated with HDL, and its expression was enriched in *Cdkal1* KO mice.

To estimate the functional roles of differentially expressed proteins, we performed KEGG analysis for associated pathways. In the case of *Cdkal1* KO mice, associations with pathways such as glyoxylate and dicarboxylate metabolism, propanoate metabolism, and butanoate metabolism were identified (Table 2). Differentially expressed proteins and network gene sets were identified in mice with *Cdkal1* deletion to identify relevant pathways. Significance was limited to a false discovery rate (FDR) < 0.05.

To investigate at what step the effect of *Cdkal1* KO on CYP3A11 is regulated, we performed a correlation analysis of *Cdkal1* and *Cyp3a11* at the mRNA level. Corresponding to the results of the proteomic analysis, *Cdkal1* and *Cyp3a11* expression were negatively correlated with each other (Figure 5). Thus, the effect of *Cdkal1* on *Cyp3a11* begins at the mRNA expression level.

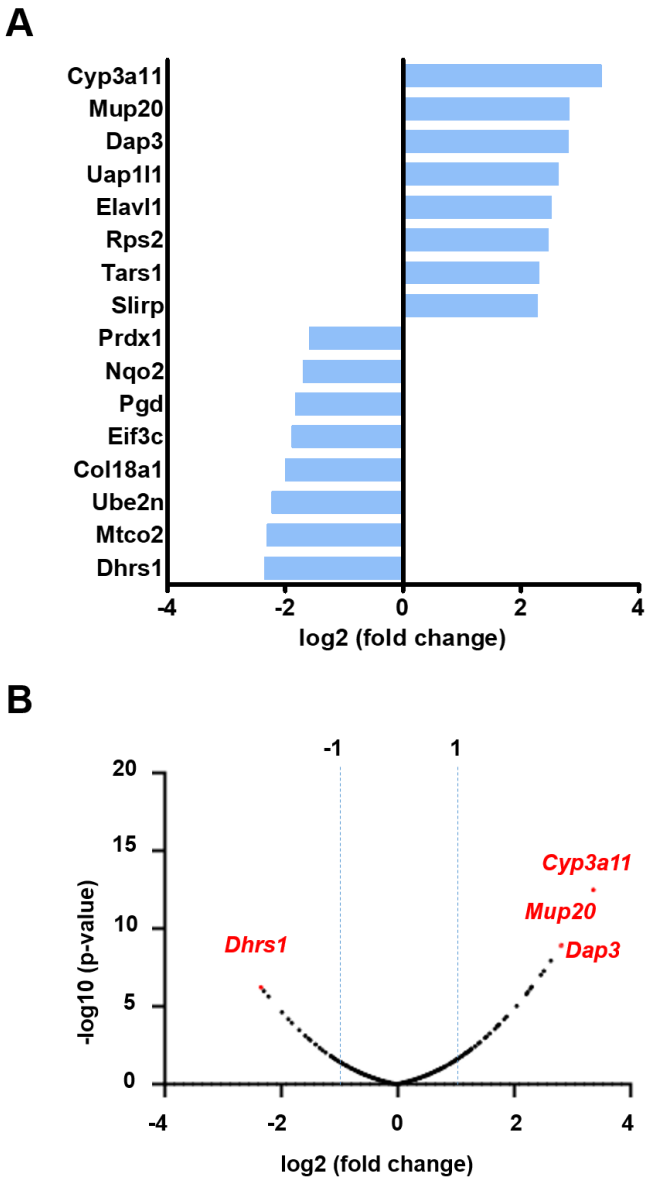

Figure 4 legend (the following page)

Figure 4. Bar and volcano plots comparing liver proteomes of *Cdkal1* KO mice to *Cdkal1*$^{fl/fl}$ mice. (A) The vertical axis represents differentially expressed proteins from different proteome categories and the horizontal axis represents the protein enrichment scores [−log2(fold change)]. Enriched differentially expressed protein significances are presented as p values < 0.05. (B) Differences in peptide abundance were evaluated between floxed and *Cdkal1* gene-deleted mouse liver. The x-axis represents the intensity ratio of peptides in the two groups of subjects, the y-axis indicates the p-value representing significance based on repetition, and each point in the plot represents the expression of an individual protein. Red indicates upregulated and downregulated proteins.

Table 2. Differentially expressed proteins and associated pathways in *Cdkal1* KO mice compared to *Cdkal1*$^{fl/fl}$ mice

A

Proteins	Genes	log2 fold change	*p*
Cytochrome P450 3A11	*Cyp3a11*	3.36	3.27E-13
Major urinary protein 20	*Mup20*	2.81	1.14E-09
Small ribosomal subunit protein mS29	*Dap3*	2.80	1.27E-09
UDP-N-acetylhexosamine pyrophosphorylase-like protein 1	*Uap1l1*	2.63	1.16E-08
ELAV-like protein 1	*Elavl1*	2.51	5.25E-08
Small ribosomal subunit protein uS5	*Rps2*	2.46	9.44E-08
Threonine--tRNA ligase 1, cytoplasmic	*Tars1*	2.30	5.61E-07
SRA stem-loop-interacting RNA-binding protein, mitochondrial	*Slirp*	2.28	7.25E-07
Peroxiredoxin-1	*Prdx1*	-1.59	7.65E-04
Ribosyldihydronicotinamide dehydrogenase [quinone]	*Nqo2*	-1.69	3.32E-04
6-phosphogluconate dehydrogenase, decarboxylating	*Pgd*	-1.82	1.12E-04
Eukaryotic translation initiation factor 3 subunit C	*Eif3c*	-1.88	6.79E-05
Isoform 2 of Collagen alpha-1(XVIII) chain	*Col18a1*	-1.99	2.36E-05
Ubiquitin-conjugating enzyme E2 N	*Ube2n*	-2.22	2.31E-06
Cytochrome c oxidase subunit 2	*Mtco2*	-2.30	1.01E-06

B

KEGG Pathways	Count in network	False discovery rate
Glyoxylate and dicarboxylate metabolism	4 of 32	1.40E-03
Propanoate metabolism	4 of 34	1.40E-03
Butanoate metabolism	3 of 28	1.74E-02
Linoleic acid metabolism	3 of 47	4.30E-02
Ribosome	8 of 127	2.00E-05
Tryptophan metabolism	3 of 51	4.89E-02
Carbonmetabolism	7 of 122	1.50E-04
Steroid hormone biosynthesis	4of 86	2.91E-02
Retinol metabolism	4 of 92	3.24E-02
Chemical carcinogenesis	4 of 97	3.48E-02
Metabolic pathways	30 of 1536	4.05E-10

Table 2 legend (the following page)

(A) Analysis of proteins affected by liver-specific *Cdkal1* deletion compared to *Cdkal1*$^{fl/fl}$ mice. Expression levels are indicated as log2 fold change and p-values. (B) KEGG pathway analysis of upregulated and downregulated proteins. The significance of enriched KEGG pathways is presented as FDR. The data were analyzed by String version 12.0 bioinformatics tools.

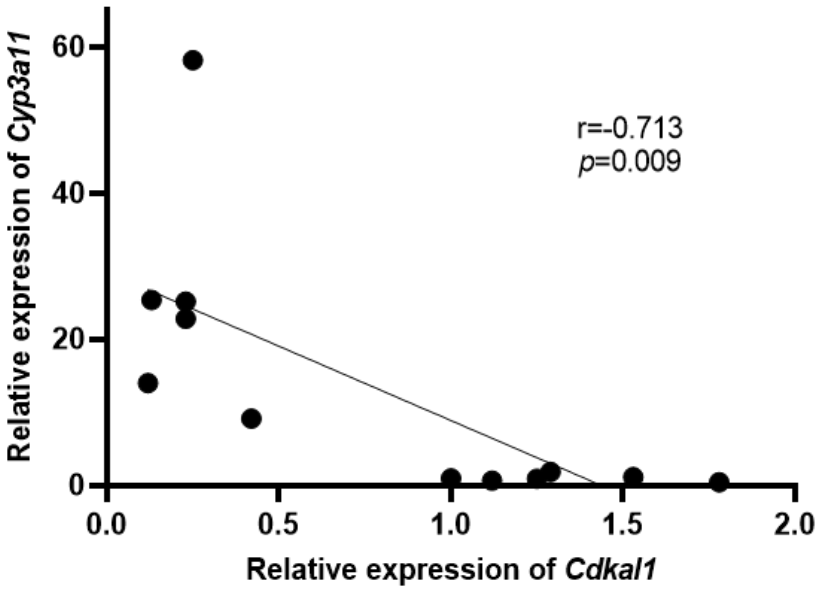

Figure 5. Correlation analysis of *Cdkal1* and *Cyp3a11* mRNA levels. In mice, the expression of *Cdkal1* and *Cyp3a11* is negatively correlated with each other. The x-axis and y-axis show the expression level of each gene as a fold change value, respectively. The correlation coefficient and p-value were obtained through correlation analysis using the Pearson correlation coefficient (n=12).

IV. DISCUSSION

The major findings of the current study are as follows: 1) hepatic *Cdkal1* deletion promoted RCT in our mouse model, and 2) diverse proteins including CYP3A11 were regulated in the liver-specific *Cdkal1* KO mice. These results demonstrate the biological effect of *Cdkal1* in the liver and provide mechanistic insight into previous human genetic data.

In our vivo study using *Cdkal1*-deleted mice, *Cdkal1* deficiency significantly affected fecal bile acids and cholesterol excretion. Additionally, although there were no changes in the liver and plasma, RCT confirmed that cholesterol excretion in the stool increased when *Cdkal1* was deficient. These results indicate that *Cdkal1* affects RCT and suggest that *Cdkal1* deficiency promotes cholesterol excretion into the feces.

Other studies have shown that mouse *Cdkal1* acts as a methylthiolase that converts t6A to ms2t6A in tRNALys(UUU)[10]. These findings provide insight into the specific biochemical functions of *Cdkal1* and its potential involvement in processes such as translation and cellular functions. However, the mechanism by which *Cdkal1* regulates RCT has not been confirmed. Key factors in RCT are APOA1, SR-B1, and HDL[5]. This may support the central role of HDL metabolism in RCT. Several studies have reported that endothelial lipase (EL) and hepatic lipase

(HL) play a role in HDL metabolism[13,14]. HL regulates HDL-C levels and functions in RCT, while EL promotes the conversion of HDL components and may function in HDL catabolism[15,16]. In our study, the most differentially expressed protein due to gene deficiency was CYP3A11. CYP3A11 is involved in bile acid metabolism and has been reported to affect HDL-C levels[17]. We propose that the mechanism by which *Cdkal1* regulates RCT may be related to HDL metabolism, possibly affecting the expression of associated proteins.

Therefore, *Cdkal1* deficiency affects RCT by a novel mechanism, which will play an important role in the development of new therapeutic strategies, whether alone or in combination with other drugs. Although we could not confirm which factors complement the effect of *Cdkal1* on cholesterol reabsorption, this study may suggest a new strategy for the prevention and treatment of atherosclerosis and dyslipidemia by revealing the potential effect of *Cdkal1* on these conditions via RCT.

In our proteomic analysis to determine the role of *Cdkal1* in cholesterol metabolism, CYP3A11 expression was the most increased. CYP3A11 is well-known to be involved in bile acid metabolism and inhibition[17,20]. As a factor that CYP3A11 relieves bile acid accumulation, it is relevant that RCTs were promoted in our study.

In the liver, cholesterol is metabolized through the *Cyp7a1* or *Cyp27a1* pathway. *Cyp27a1*$^{-/-}$ mice have increased activity of CYP3A, an enzyme that can hydroxylate sterols and bile acid intermediates[18,19]. These metabolites can be excreted from the body in the bile or urine. Additionally, increased expression of hepatic cytochrome P450 *Cyp3a11,* which is involved in bile acid detoxification, reportedly contributes to the anti-atherosclerotic mechanism by decreasing total cholesterol and LDL-C and increasing HDL-C[17]. Our findings expand previous work by suggesting that *Cyp3a11* promotes cholesterol excretion.

Pathway analysis of mice revealed that glyoxylate and dicarboxylate metabolism as well as carbon metabolism were involved. In several studies conducted to discover metabolomic biomarkers of CVDs and their risk, glyoxylate and dicarboxylate metabolism and aminoacyl-tRNA biosynthesis were highly significant[21,22]. These findings suggest that the *Cdkal1* gene in mice is related to CVDs and is a potential therapeutic target. The role of *Cdkal1* in RCT and CVD will be better understood as further validation and studies are conducted on the proteins and the mechanisms regulated in the pathway.

A limitation of this study is that it did not determine whether the differentially expressed proteins identified in proteomic analysis affected RCT. To confirm this, it is first necessary to analyze differentially expressed factors in *Cdkal1* KO mice

at the protein level. These analyses serve as the basis for proteomic analysis and can be a starting point for identifying the role of *Cdkal1* in RCT and the mechanisms involved. Our study found that liver-specific *Cdkal1* deficiency improves RCT, but the mechanisms involved are unclear. We found that CYP3A11, a protein that functions in HDL-C and bile acid metabolism, was most affected by *Cdka11* deficiency, but its effect on RCT is unclear. Our results showed changes in bile acids and cholesterol in fecal excretion, a finding that needs to be confirmed. If CYP3A11 is confirmed to be up-regulated in *Cdkal1* KO mice, it will be necessary to knock down this protein using methods such as shRNA or CRISPR, or to produce double KO mice to analyze the effects of this protein on RCT. Finding downstream pathways can broaden the coverage of *Cdkal1* and help uncover new functions.

In conclusion, our findings contribute to understanding the role of *Cdkal1* in cholesterol metabolism and its impact on RCT. Identifying *Cdkal1* as a potential therapeutic target opens avenues for further research into interventions for metabolic and atherosclerotic vascular diseases.

V. CONCLUSION

Our study confirmed that liver-specific *Cdkal1* deficiency affects RCT. Liver-specific *Cdkal1* deficiency affected bile acids and cholesterol in fecal excretion. Proteomic analysis suggested potential targets included in pathways affected by *Cdkal1*. Our study provides a new research direction for the *Cdkal1*.

REFERENCE

1. Mc Namara K, Alzubaidi H, Jackson JK. Cardiovascular disease as a leading cause of death: how are pharmacists getting involved? Integr Pharm Res Pract 2019;8:1-11.

2. Ouimet M, Barrett TJ, Fisher EA. HDL and reverse cholesterol transport. Circ Res 2019;124:1505-1518.

3. Favari E, Chroni A, Tietge UJ, Zanotti I, Escolà-Gil JC, Bernini F. Cholesterol efflux and reverse cholesterol transport. Handb Exp Pharmacol 2015;224:181-206.

4. Pownall HJ, Rosales C, Gillard BK, Gotto AM Jr. High-density lipoproteins, reverse cholesterol transport and atherogenesis. Nat Rev Cardiol 2021;18:712-723.

5. van der Velde AE. Reverse cholesterol transport revisited. World J Gastroenteerol 2010;16:5907.

6. Marques LR, Diniz TA, Antunes BM, Rossi FE, Caperuto EC, Lira FS et al. Reverse Cholesterol Transport: Molecular Mechanisms and the Non-medical Approach to Enhance HDL Cholesterol. Front Physiol 2018;9:526.

7. Zhang Y, Zanotti I, Reilly MP, Glick JM, Rothblat GH, Rader DJ. Overexpression of apolipoprotein A-I promotes reverse transport of cholesterol from macrophages to feces in vivo. Circulation 2003;108:661-3.

8. Cuchel M, Raper AC, Conlon DM, Pryma DA, Freifelder RH, Poria R et al. A novel approach to measuring macrophage-specific reverse cholesterol transport in vivo in humans. J Lipid Res 2017;58:752-762.

9. Palmer CJ, Bruckner RJ, Paulo JA, Kazak L, Long JZ, Mina AI et al. *Cdkal1*, a type 2 diabetes susceptibility gene, regulates mitochondrial function in adipose tissue. Mol Metab 2017;6:1212-1225.

10. Wei FY, Suzuki T, Watanabe S, Kimura S, Kaitsuka T, Fujimura A et al. Deficit of tRNA(Lys) modification by *Cdkal1* causes the development of type 2 diabetes in mice. J Clin Invest 2011;121:3598-608.

11. Cheon EJ, Cha DH, Cho SK, Noh HM, Park S, Kang SM et al. Novel association between *CDKAL1* and cholesterol efflux capacity : replication after GWAS-based discovery. Atherosclerosis 2018;273, 21–27.

12. Saini RK, Prasad P, Shang X, Keum YS. Advances in lipid extraction methods—A review. Int J Mol Sci 2021;22:13643.

13. Cohen JC. Endothelial lipase: direct evidence for a role in HDL metabolism. J Clin Invest 2003;111:318-21.

14. Connelly PW, Hegele RA. Hepatic lipase deficiency. Crit Rev Clin Lab Sci 1998;35:547-72.

15. Jaye M, Krawiec J. Endothelial lipase and HDL metabolism. Curr Opin Lipidol 2004;15:183-9.

16. Thuren T. Hepatic lipase and HDL metabolism. Curr Opin Lipidol 2000;11:277-83.

17. Hashimoto M, Kobayashi K, Watanabe M, Kazuki Y, Takehara S, Inaba A et al. Knockout of mouse *Cyp3a* gene enhances synthesis of cholesterol and bile acid in the liver. J Lipid Res 2013;54:2060-2068.

18. Hall E, Hylemon P, Vlahcevic Z, Mallonee D, Valerie K, Avadhani N et al. Overexpression of *CYP27* in hepatic and extrahepatic cells: role in the regulation of cholesterol homeostasis. Am J Physiol Gastrointest Liver Physiol 2001;281:G293-301.

19. Zurkinden L, Solcà C, Vögeli IA, Vogt B, Ackermann D, Erickson SK et al. Effect of *Cyp27A1* gene dosage on atherosclerosis development in ApoE-knockout mice. FASEB J 2014;28:1198-209.

20. Goodwin B, Gauthier KC, Umetani M, Watson MA, Lochansky MI, Collins JL et al. Identification of bile acid precursors as endogenous ligands for the nuclear xenobiotic pregnane X receptor. Proc Natl Acad Sci USA 2003;100:223-8.

21. Zou Y, Yang Y, Fu X, He X, Liu M, Zong T et al. The regulatory roles of aminoacyl-tRNA synthetase in cardiovascular disease. Mol Ther Nucleic Acids 2021;24:25:372-387.

22. Chen G, Ye G, Zhang X, Liu X, Tu Y, Ye Z et al. Metabolomics Reveals Protection of Resveratrol in Diet-Induced Metabolic Risk Factors in Abdominal Muscle. Cell Physiol Biochem. 2018;45:1136-1148.

ABSTRACT (IN KOREAN)

간 *Cdkal1* 과 콜레스테롤 역수송

<지도교수 이상학>

연세대학교 대학원 생체공학협동과정

석승민

Cdkal1 유전자는 고밀도 지단백질 기능의 지표이자 콜레스테롤 역수송 (RTC)의 첫 번째 단계인 콜레스테롤 유출 용량과 관련된 유전자좌 근처에 있다. 여기서는 마우스 모델을 사용하여 RCT 에 대한 *Cdkal1* 의 효과를 조사했다. 거품 세포를 ^{3}H 표지된 콜레스테롤로

처리하고 마우스에 복강내 주사했다. 48 시간 후 혈장, 간, 대변을 채취하고 액체섬광계수기를 이용하여 방사능을 측정했다.

Cdka11 의 효과와 잠재적으로 관련이 있는 단백질 및 경로를 확인하기 위해 마우스 단백체 분석을 수행했다. 마우스 간 단백질을 추출하고 액체 크로마토그래피-질량 분석법을 사용하여 분석했다.

간 특이적 *Cdka11* 결핍 마우스는 $Cdka11^{fl/fl}$ 마우스를 *Alb-Cre* 마우스와 교배하여 생산했다. RCT 실험에서는 *Cdka11* 결핍이 분변 담즙산 및 콜레스테롤 배설에 영향을 미치는 것으로 나타났는데, $Cdka11^{fl/fl}$ 마우스에 비해 *Cdka11* 녹아웃 (KO) 마우스에서 담즙산이 17% (p=0.035) 더 높고 콜레스테롤이 42% (p=0.036) 더 높았다.

Cdka11 KO 마우스를 $Cdka11^{fl/fl}$ 마우스와 비교하는 단백체 분석을 통해 CYP3A11 을 포함하여 차등적으로 발현되는 여러 단백질을 확인했다.

결론적으로 간 특이성 *Cdka11* 결핍은 마우스 모델에서 RCT 를 촉진했다. 단백체 분석을 통해 CYP3A11 을 포함하여 *Cdka11* 의 결핍과 잠재적으로 연관된 단백질을 확인했다. 이러한 결과는 *Cdka11* 이

대사성 및 죽상경화성 혈관 질환에 대한 잠재적인 치료 표적이 될 수 있음을 시사한다.

핵심되는 말: 콜레스테롤 역수송, 간, 단백체학, 동맥경화